Figure S1

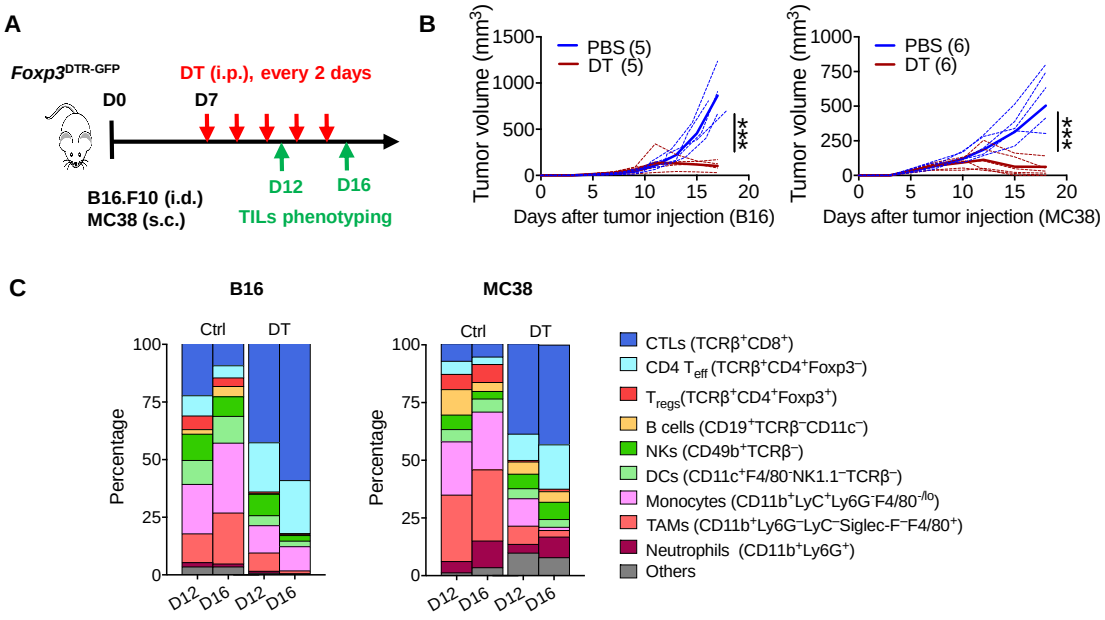

Figure S1. Impact of transient T_{regs} depletion on the cellular composition of the TME (Related to Figure 1).

(A) Scheme of T_{reg} depletion induced by diphtheria toxin (DT) treatment in *Foxp3*$^{DTR\text{-}GFP}$ mice implanted with B16.F10 (B16) melanoma or MC38 colon adenocarcinoma tumors. **(B)** *Foxp3*$^{DTR\text{-}GFP}$ mice were injected with B16 ($1.25x10^5$, i.d.) or MC38 ($2.5x10^5$, s.c.) on D0. DT (250 ng) or vehicle (PBS) was injected (i.p) every 2 days starting on D7 (when tumors are palpable) for a total of 5 doses. Tumor growth measured every 3 days with a digital caliper. ***p<0.001; (Two-way ANOVA with p value corrected for multiple comparison). **(C)** Flow cytometric phenotyping of different immune cell types present in the TME of B16 or MC38 tumor-bearing *Foxp3*$^{DTR\text{-}GFP}$ mice after 3 doses (D12) or 5 doses (D16) DT or PBS injection (i.p.). Data are presented as the percentage of individual cell populations in the $CD45^+$ cells. The surface markers used to define each cell subset are indicated. n=3-5 for each time point.

Figure S2

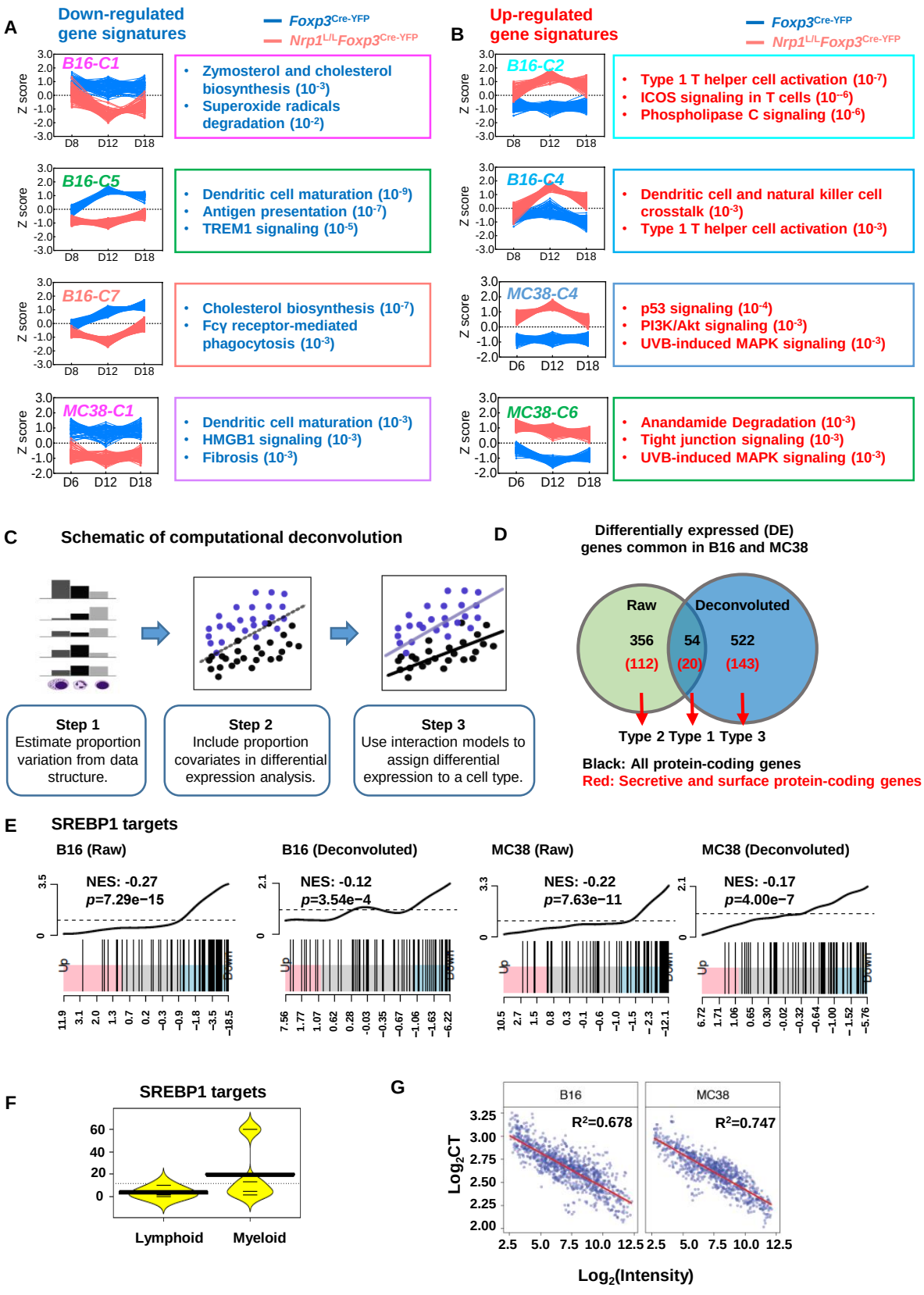
A
Down-regulated gene signatures
Foxp3Cre-YFP
Nrp1L/LFoxp3Cre-YFP
B16-C1
• Zymosterol and cholesterol biosynthesis (10-3)
• Superoxide radicals degradation (10-2)
B16-C5
• Dendritic cell maturation (10-9)
• Antigen presentation (10-7)
• TREM1 signaling (10-5)
B16-C7
• Cholesterol biosynthesis (10-7)
• Fcγ receptor-mediated phagocytosis (10-3)
MC38-C1
• Dendritic cell maturation (10-3)
• HMGB1 signaling (10-3)
• Fibrosis (10-3)
B
Up-regulated gene signatures
Foxp3Cre-YFP
Nrp1L/LFoxp3Cre-YFP
B16-C2
• Type 1 T helper cell activation (10-7)
• ICOS signaling in T cells (10-6)
• Phospholipase C signaling (10-6)
B16-C4
• Dendritic cell and natural killer cell crosstalk (10-3)
• Type 1 T helper cell activation (10-3)
MC38-C4
• p53 signaling (10-4)
• PI3K/Akt signaling (10-3)
• UVB-induced MAPK signaling (10-3)
MC38-C6
• Anandamide Degradation (10-3)
• Tight junction signaling (10-3)
• UVB-induced MAPK signaling (10-3)
Z score
D8 D12 D18
D6 D12 D18
C
Schematic of computational deconvolution
Step 1
Estimate proportion variation from data structure.
Step 2
Include proportion covariates in differential expression analysis.
Step 3
Use interaction models to assign differential expression to a cell type.
D
Differentially expressed (DE) genes common in B16 and MC38
Raw
Deconvoluted
356
(112)
54
(20)
522
(143)
Type 2 Type 1 Type 3
Black: All protein-coding genes
Red: Secretive and surface protein-coding genes
E
SREBP1 targets
B16 (Raw)
NES: -0.27
p=7.29e−15
B16 (Deconvoluted)
NES: -0.12
p=3.54e−4
MC38 (Raw)
NES: -0.22
p=7.63e−11
MC38 (Deconvoluted)
NES: -0.17
p=4.00e−7
Up
Down
F
SREBP1 targets
Lymphoid
Myeloid
G
B16
MC38
R²=0.678
R²=0.747
Log2CT
Log2(Intensity)

Figure S2. T_{regs} shape the transcriptional landscape of tumor-infiltrating immune cells (Related to Figure 2).
(**A, B**) Co-expression clusters (*K*-means) for genes that were (A) up- or (B) down-regulated in tumor-infiltrating $CD45^+$ cell transcriptome from *Nrp1*$^{L/L}$*Foxp3*$^{Cre\text{-}YFP}$ mice compared to *Foxp3*$^{Cre\text{-}YFP}$ mice. Gene Ontology (GO) analysis of top enriched biological pathways for the selected gene clusters are shown in the boxes. Number in parenthesis indicated P value for enrichment. Font color indicated direction of regulation (Red: up-regulated; Blue: down-regulated). **(C)** Scheme for the method of computational deconvolution. **(D)** Venn diagram depiction of the patterns (Type 1-3) of differential expression and selection criteria for candidates included in Fluidigm validation. **(E)** Gene Set Enrichment Analysis (GSEA) assessing the modulation of SREBP1 targets in the tumor-infiltrating $CD45^+$ transcriptome derived from B16 or MC38 tumor models (as in Figure 2A-F), both in raw and deconvoluted datasets. **(F)** Cell type assignment for the modulation of SREBP1 targets between lymphoid and myeloid cells in $CD45^+$ transcriptome. **(G)** Comparison of expression levels measured by Fluidigm (Y axis, values for cycle threshold (CT), log2 transformed) and microarray (X axis, intensity, log2 transformed) on the selected 80 genes (Table S1). Expression values for Fluidigm were normalized by the average of four housekeeping control genes.

Figure S3

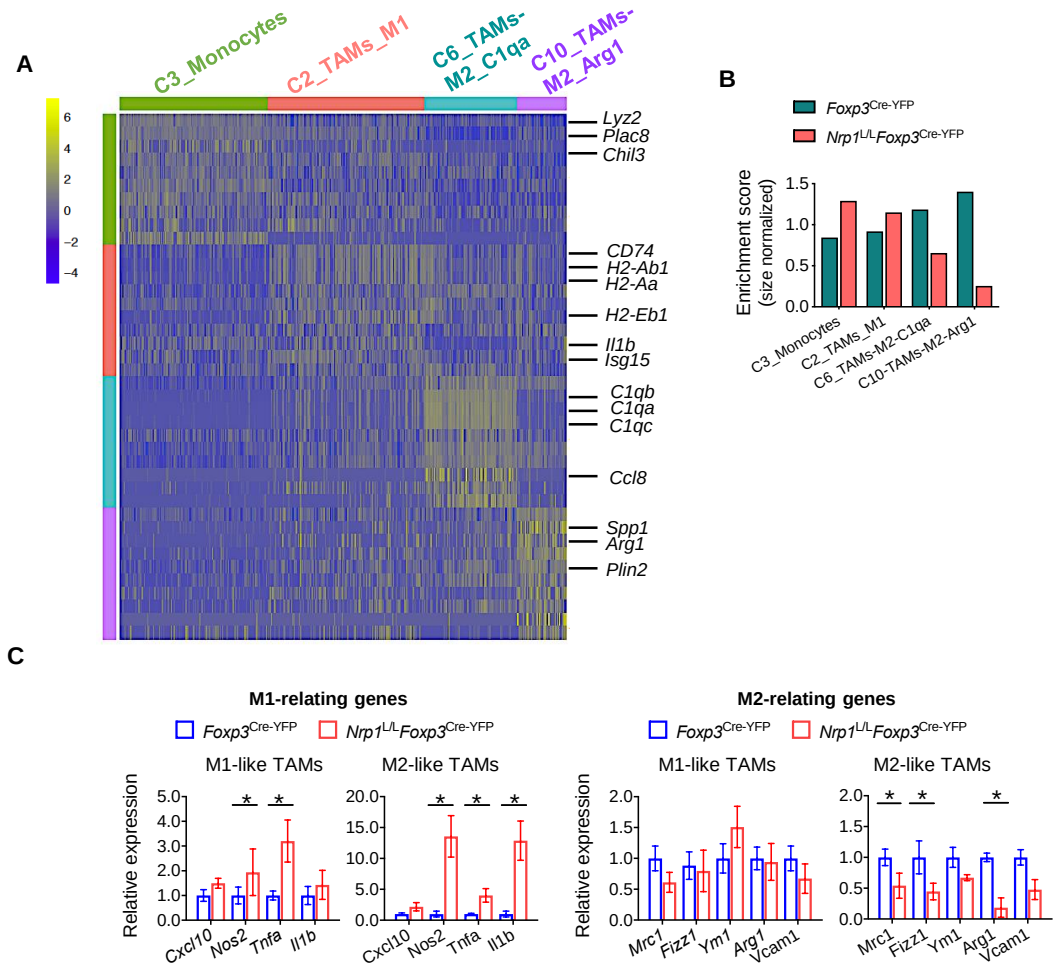

Figure S3. Functional T_{regs} are required to promote an M2-like TAM phenotype. (Related to Figure 3)

(A) Heatmap depicting the top 10 differentially expressed genes in the monocyte/macrophages- derived single cell clusters by scRNAseq ; **(B)** Relative contribution of cells originated from *Foxp3*$^{Cre\text{-}YFP}$ and *Nrp1*$^{L/L}$*Foxp3*^{Cre} mice to each of the single cell cluster (indicated), calculated by an ”enrichment score” after normalizing the input of each genotype to the total monocyte/macrophage compartment. **(C)** Analysis of selected M1- and M2- relating genes by qPCR in MHCII^{hi} TAMs (M1-like) and MHCII^{lo} TAMs (M2-like) purified from B16 tumors. Data were pooled from 3 independent experiments with n=6-7 for each genotype. Unpaired Student’s *t* test. (*P<0.05)

Figure S4

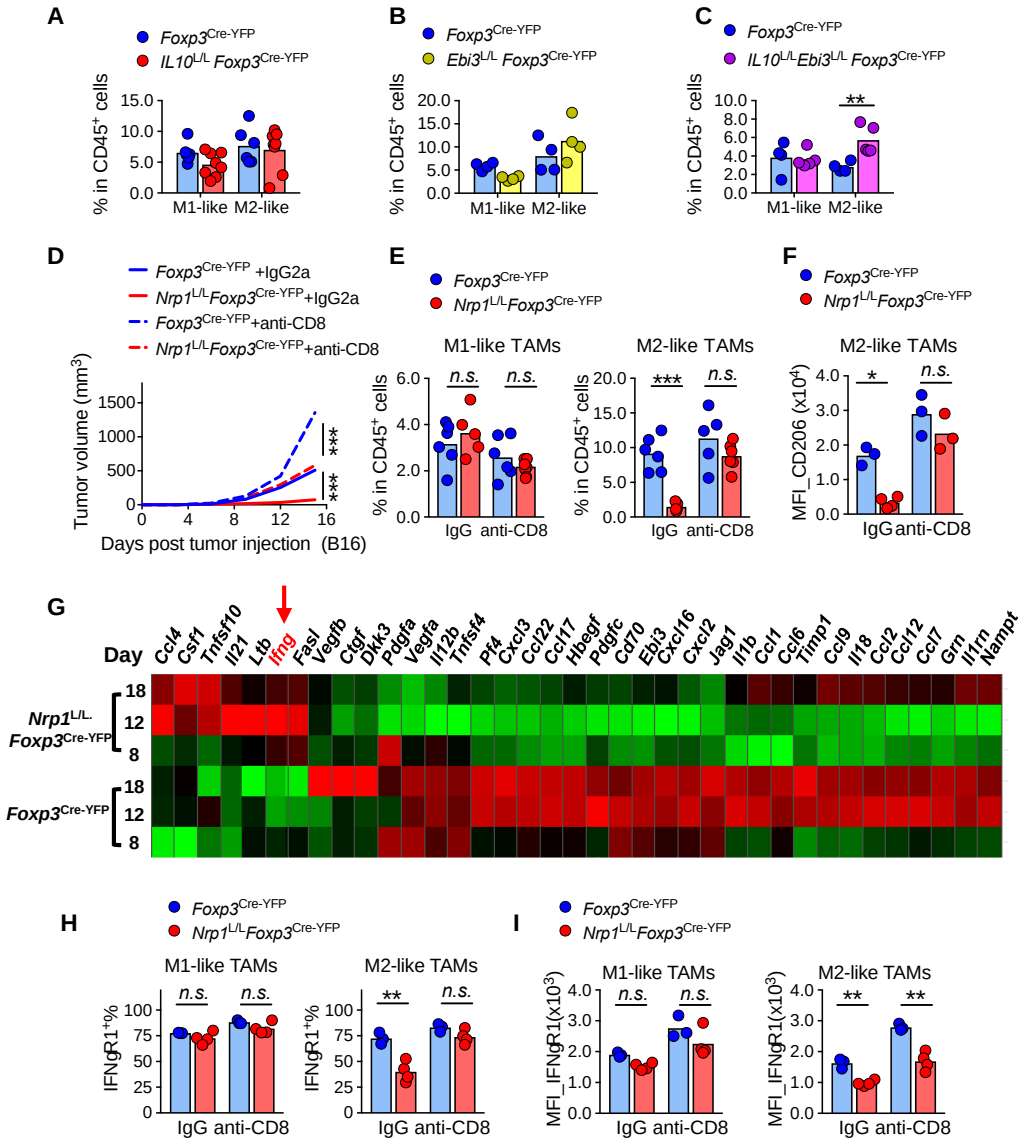

Figure S4. T_{regs} promote M2-like TAMs indirectly by repressing CD8⁺ T cell- IFNγ axis (Related to Figure 4).

(A-C) Percentage of M1-like and M2-like TAMs in tumor-infiltrating CD45⁺ cells in the B16 tumors implanted in (A) *Il10*$^{L/L}$*Foxp3*$^{Cre\text{-}YFP}$ mice; (B) *Ebi3*$^{L/L}$*Foxp3*$^{Cre\text{-}YFP}$ mice; and (C) *Il10*$^{L/L}$*Ebi3*$^{L/L}$*Foxp3*$^{Cre\text{-}YFP}$, compared to that from the *Foxp3*$^{Cre\text{-}YFP}$ control mice, respectively (n=4-6). (**D-F**) *Foxp3*$^{Cre\text{-}YFP}$ and *Nrp1*$^{L/L}$*Foxp3*$^{Cre\text{-}YFP}$ mice were treated with a CD8-depleting antibody (53.6-7) or isotype control (Rat IgG2a) every 3 days started on D0 of B16 tumor implantation. Tumors were harvested on D16 for analysis. (D) Tumor growth curves for the indicated groups. (n=6-9 for each group, 2 experiments.) (E) Percentages of M1-like and M2-like TAMs in tumor-infiltrating CD45⁺ cells. (n=5) (F) Expression (by geometric mean fluorescence intensity (MFI)) of CD206 by M2-like TAMs. (n=3-4); (**G**) Heatmap illustration for the differentially expressed genes encoding secretive/membrane proteins by B16 tumor-infiltrating CD45⁺ cells from the *Foxp3*$^{Cre\text{-}YFP}$ or *Nrp1*$^{L/L}$*Foxp3*$^{Cre\text{-}YFP}$ mice, on D8/D12/D18 post tumor inoculation. **(H, I)** (H) Percentage of IFNγR1⁺ and (I) MFI for IFNγR1 within M1-like and M2-like TAMs subset, respectively (n=4). Two-way ANOVA (**P<0.01).

Figure S5

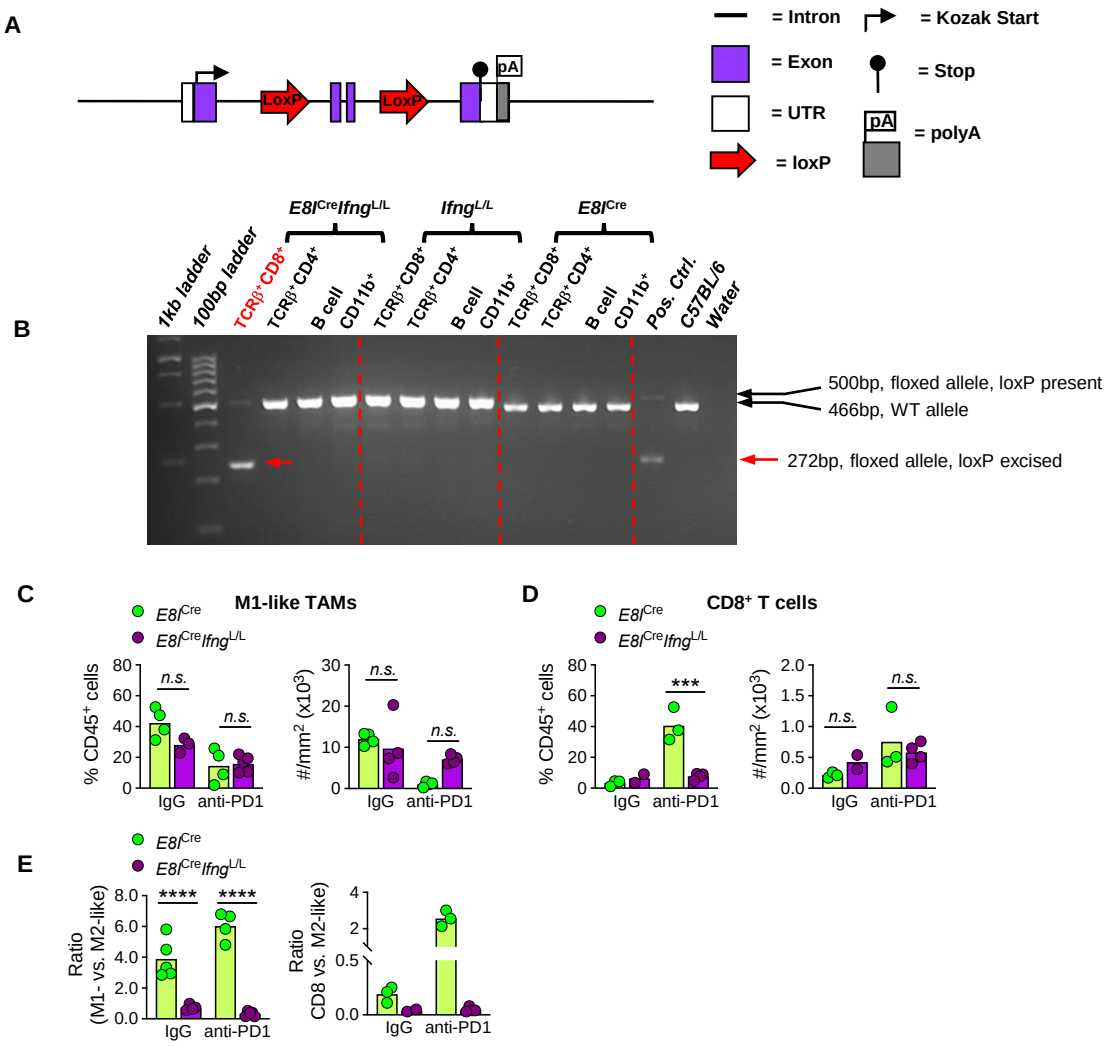

Figure S5. CD8-restrictive deletion of *Ifng* drives resistance to anti-PD1 treatment in MC38 tumor model. (Related to Figure 4).

(A) Map for the targeted allele in the *Ifng*$^{L/L}$ mice. 5' and 3' loxP site was inserted in the Intron 1 and 3 of the mouse *Ifng* gene (NM_008337.4) locus by the CRISPR/Cas9 technology (See **STAR Methods**). **(B)** Validation of CD8-restricted *Ifng* gene deletion at genomic DNA level. CD8$^+$, CD4$^+$ T cells, B cells (B220$^+$CD19$^+$) and myeloid cells (CD11b$^+$) were purified from spleen of the *E8I*^{Cre}*Ifng*$^{L/L}$, *Ifng*$^{L/L}$ and *E8I*^{Cre} mice. End-point PCR was performed with primers designed to distinguish the foxed allele, either with loxP sequence present (500bp) or excised (272 bp), or the WT allele (466bp). **(C-E)** The *E8I*^{Cre} or *E8I*^{Cre}*Ifng*$^{L/L}$ mice were inoculated with 5x10^5 MC38 tumors (s.c.), followed by anti-PD1 (clone 29F.1A12) or Rat IgG2a control (IgG) treatment on D6/D9/D12. *Ex vivo* TILs analysis was performed on D18. Bar graph tabulating the percentage (within the CD45$^+$ cells) and the cell counts per mm^2 tumor for (C) M1-like TAMs and (D) CD8$^+$ T cells; (E) The ratios for M1-/M2- like TAMs, and CD8/M2-like TAMs. (n=3-5 per group) Two-way ANOVA (****P<0.0001, ***P<0.001).

Figure S6

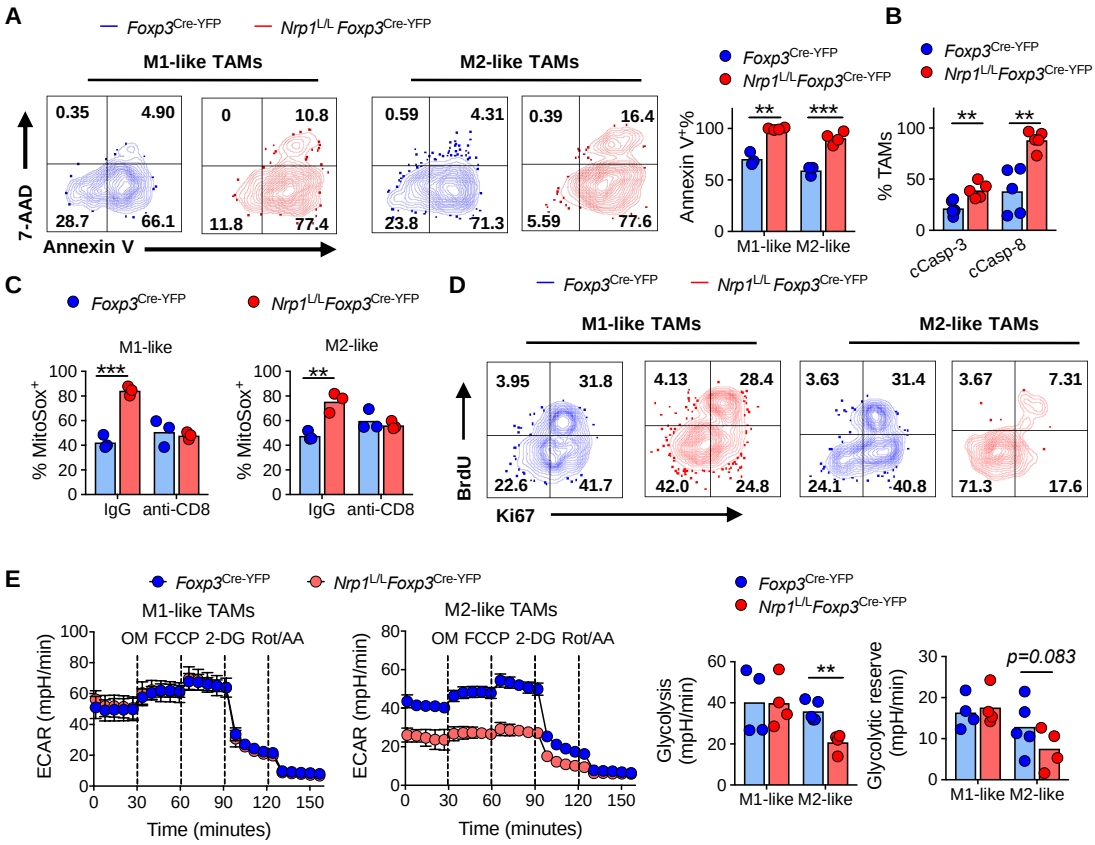

Figure S6. *Nrp1*$^{-/-}$ T_{regs} promote increased cell death and reduced proliferation of M2-like TAMs (Related to Figure 5).

B16 tumors from *Nrp1*$^{L/L}$*Foxp3*$^{Cre\text{-}YFP}$ and *Foxp3*$^{Cre\text{-}YFP}$ mice were harvested on D18 after implantation for direct *ex vivo* analysis. **(A)** Annexin V and 7-AAD staining was performed followed by flow cytometric analysis. Cells were gated on M1-like and M2-like TAMs and the percentage of total Annexin V^{+} cells within each subset was plotted. Data pooled from 2 independent experiments (n=6). **(B)** Percentages of cells in TAMs that were positive for Caspase-3 and Caspase-8 activity, respectively. Data were pooled from 2 independent experiment (n=6). **(C)** Percentage of MitoSox^{+} cells within M1- and M2-like TAMs from mice subjected to CD8 depletion, as in Figure 4 (n=3). **(D)** 5-Bromo-2'-deoxyuridine (BrdU) was injected (2mg, i.p.) 12 hours prior to tumor harvest. Representative flow cytometric plots were shown for the detection of Ki67 and BrdU, gated on M1-like, and M2-like TAMs, respectively. **(E)** Measurement of extracellular acidification rate (ECAR) of the sorted TAMs subsets. Basal glycolysis rate and glycolytic reserve were plotted (n=4). Two-way ANOVA for (C) and Unpaired Student's *t* test for (A, B, E). (***P<0.001, **P<0.01). Error bars indicate SEM from biological replicates.

Figure S7

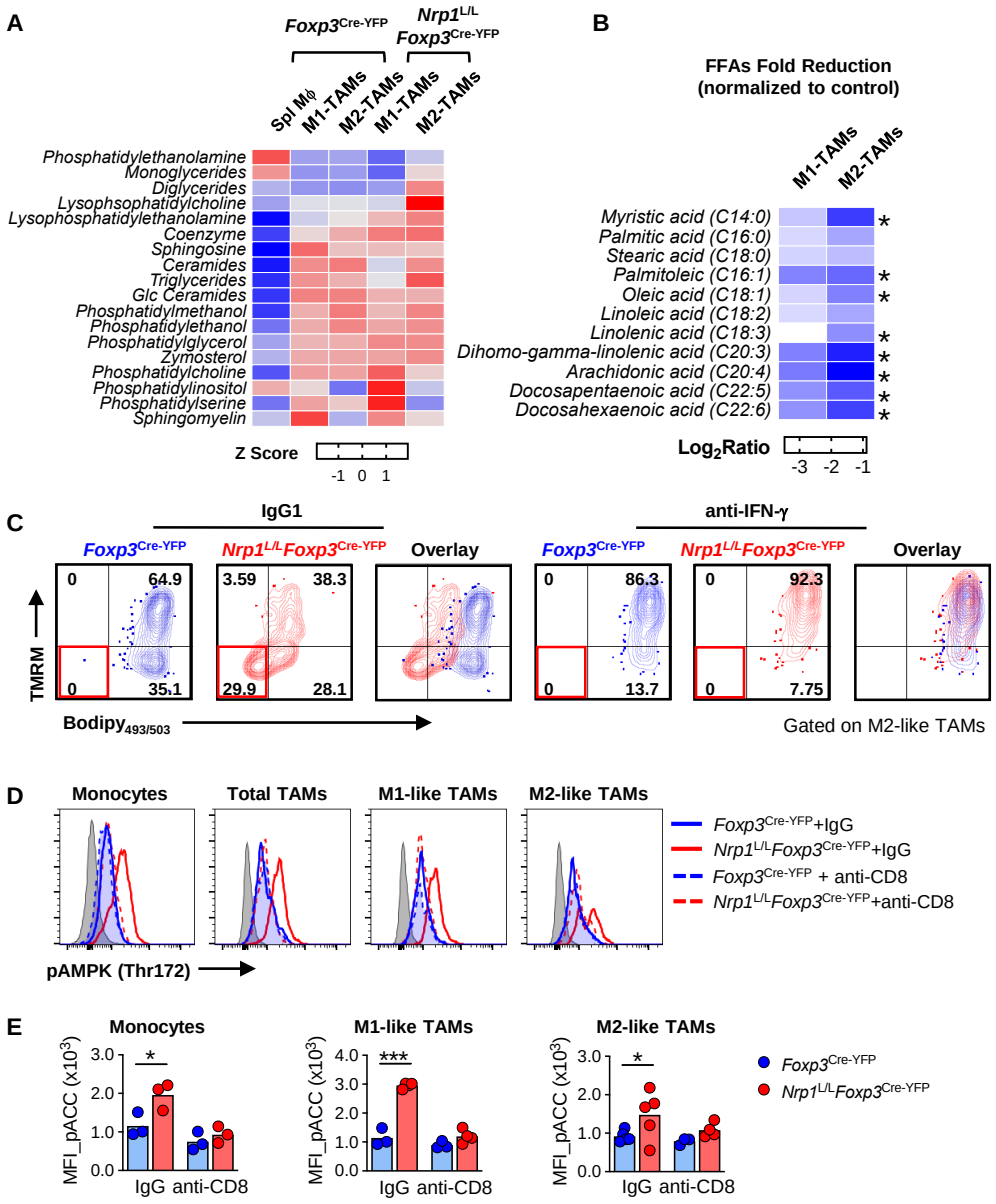

Figure S7. Impact of *Nrp1*$^{-/-}$ T_{regs} on the lipid metabolism of TAMs. (Related to Figure 6).

(A, B) Lipidome profiling of TAM subsets and splenic F4/80^{+}Ly6C^{-} macrophages, sorted from B16-bearing *Foxp3*$^{Cre\text{-}YFP}$ and *Nrp1*$^{L/L}$*Foxp3*$^{Cre\text{-}YFP}$ mice on D18 after inoculation. Heatmap depiction for (A) 18 major lipid classes (z-score transformed) across the indicated sample groups, and (B) the fold reduction (log_2 transformed) of free fatty acids species in M1-like and M2-like TAMs from the *Nrp1*$^{L/L}$*Foxp3*$^{Cre\text{-}YFP}$ mice, compared to their counterparts from the *Foxp3*$^{Cre\text{-}YFP}$ mice (control). Species marked by the star symbol (*) indicated more than 4 fold (–log2ratio≥ 2) reduction in at least one TAM subset. **(C)** B16 tumors were harvested on D20 from *Foxp3*$^{Cre\text{-}YFP}$ and *Nrp1*$^{L/L}$*Foxp3*$^{Cre\text{-}YFP}$ mice subjected to the IFNγ neutralization experiment (as in Fig. 4A), and co-stained with Bodipy$_{493/503}$ and TMRM, gated on M2-like TAMs. **(D, E)** B16 tumors from mice subjected to CD8-depletion were analyzed on D16 post inoculation. Cells were stained for the phosphorylated AMP-activated protein kinase (AMPK) or phosphorylated acetyl-CoA carboxylase (ACC), followed by incubation with an APC-conjugated secondary antibody, and analyzed on a flow cytometer. (D) Representative histograms for pAMPK (Thr172); (E) MFI for pACC (Ser79) , gated on Monocytes, total TAMs, M1-like and M2-like TAMs, respectively (n=5, 2 experients). Two-way ANOVA (***P<0.001, *P<0.05)

Table S1

Differential Expression	Definition	Gene list
Type 1	Differentially expressed both in raw and deconvoluted datasets	*Il6, Fasl, Itga4, Il18r1, Cyr61,Cav1,Fcrls,Penk,C4b,Cxcl14,Tnfsf9,Adora2b,Grasp,C1r,Il18bp,Olfml3,Flt1,Chil3,Hp,F7,F10,Ltb4r, Cd80,Flrt2, Nrp2, Emr4, Il10*
Type 2	Differentially expressed only in raw datasets	*Anxa6,Cd28,Gpr174,Klre1,Itga1,Il18rap,Slamf1,Klra7,Pglyrp2,Cobll1,Spry2,Sla2,Crtam,Sell,Mpzl1,Vcam1,Fads2,Igfbp4,Slamf9,Pdgfc,Cp,Cadm1,Smo,Pltp,Htra3,Dcbld2,Bmpr1a,Cd72,Tlr7,Fads1,Vegfb,Nenf*
Type 3	Differentially expressed only in deconvolution datasets	*Ccr1, Il1r2, Cd83,Ly6e, Tnf, Calcrl, Ptger4, Gpr132, Sla, Adcy7, Tnfrsf9, Nrp1, Fcgrt, Tlr2, Pf4, Ceacam1, C5ar1, Sdc4, Icosl, Xcl1*

Table S1: Gene list for Fluidigm Biomark qPCR validation (Related to Figure 2).

The list of the 80-gene signature, grouped by how they were differentially expressed in the intratumoral CD45^{+} transcriptome profiles derived from B16 or MC38 tumor-bearing *Foxp3*$^{\text{Cre-YFP}}$ and *Nrp1*$^{\text{L/L}}$*Foxp3*$^{\text{Cre-YFP}}$ mice, determined by direct microarray measurement (raw data) and after cell composition correction (deconvoluted data). Color code indicates the direction of modulation (Red: up-regulated; Blue: down-regulated).

Table S3

Genes	RefSeq	Forward Primer (5'→3')	Reverse Primer (5'→3')
Mrc1	NM_008625.2	CTCTGTTCAGCTATTGGACGC	CGGAATTTCTGGGATTCAGCTTC
Retnla	NM_020509.3	TCGTGGAGAATAAGGTCAAGG	GGAGGCCCATCTGTTCATAG
Chi3l3	NM_009892.2	GCCCACCAGGAAAGTACACA	CCTCAGTGGCTCCTTCATTCA
Arg1	NM_007482.3	CTCCAAGCCAAAGTCCTTAGAG	AGGAGCTGTCATTAGGGACATC
Vcam1	NM_011693.3	CCCAAACAGAGGCAGAGTGTA	TGACCCAGATGGTGGTTTCC
Nos2	NM_010927.4	GTTCTCAGCCCAACAATACAAGA	GTGGACGGGTCGATGTCAC
Il1b	NM_008361.3	GAAATGCCACCTTTTGACAGTG	TGGATGCTCTCATCAGGACAG
Cxcl10	NM_021274.2	CCAAGTGCTGCCGTCATTTTC	GGCTCGCAGGGATGATTTCAA
Tnf	NM_013693.3	GGGTGATCGGTCCCCAAA	TGAGGGTCTGGGCCATAGAA
Bcl2l11	NM_207680.2	CCCGGAGATACGGATTGCAC	GCCTCGCGGTAATCATTTGC
Hspa5	NM_001163434.1	GCATCACGCCGTCGTATGT	ATTCCAAGTGCGTCCGATGAG
Ero1l	NM_015774.3	CGGACCAAGTTATGAGTTCCA	TCAGAGAGATTCTGCCCTTCA
Ddit3	NM_013760.4	GTCCCTAGCTTGGCTGACAGA	TGGAGAGCGAGGGCTTTG
Erdj4	NM_013760.4	TAAAAGCCCTGATGCTGAAGC	TCCGACTATTGGCATCCGA
Fads1	NM_146094.2	GAAGCACATGCCATACAACC	CTGGAAGTATAGAGGCAGCAA
Fads2	NM_019699.1	CACGTTGTCCACAAGTTTGTCA	TGGAAATGTCGGTGGTTCCA
Hprt	NM_013556.2	CAGTACAGCCCCAAAATGGTTA	AGTCTGGCCTGTATCCAACA

Table S3: Primer sequences for QPCR gene expression assay (Related to STAR Methods).